

# Imaging Features of Clavicular Pathologies and Their Articulations: A Pictorial Essay

**BWT Cheng, JHM Cheng, KH Chin, CY Chu**

*Department of Radiology, Pamela Youde Nethersole Eastern Hospital, Hong Kong SAR, China*

## INTRODUCTION

The clavicle, the acromioclavicular (AC) joint and the sternoclavicular joint can be affected by a wide range of pathologies, including infection, inflammation, degeneration, metabolic disorders, neoplasms, trauma, and congenital anomalies. This pictorial essay illustrates the radiological features of clavicular pathologies to facilitate accurate diagnosis and management, based on cases of clavicular, AC and sternoclavicular pathologies diagnosed in the Hong Kong East Cluster from April 2014 to April 2023.

## NORMAL ANATOMY

A basic understanding of the anatomy of the clavicle and its articulations is essential for image interpretation. The clavicle is a horizontally oriented S-shaped bone that has a large medial metaphysis articulating with the sternum, a tubular diaphysis, and a flared lateral metaphysis that articulates with the acromion (Figure 1). The sternoclavicular joint is a synovial joint formed by the medial clavicular metaphysis, the clavicular notch of the manubrium sterni, and the cartilage of

the first rib. The articular surfaces of the clavicle and manubrium are separated by a fibrocartilaginous disk.<sup>1</sup> The costoclavicular and sternoclavicular ligaments (thickenings of the joint capsule), and interclavicular ligament (located between the superomedial ends of the two clavicles) provide joint stability (Figure 2).<sup>2</sup> The AC joint is a planar diarthrodial joint located between the lateral surface of the clavicle and the medial surface of the acromion. Stabilisers of the joint include the AC joint capsule and the AC, coracoacromial, and coracoclavicular (consisting of trapezoid and conoid ligaments) ligaments. A flexible fibrocartilaginous disk is peripherally continuous with the joint capsule (Figure 3).<sup>3</sup> There are four types of acromion shape, namely, flat, curved, hooked, and convex. An unfused acromial ossification centre (os acromiale) is an anatomical variant.

## RADIOLOGICAL FEATURES OF PATHOLOGIES

### Congenital Anomalies

Cleidocranial dysostosis is a rare autosomal dominant

---

*Correspondence:* Dr BWT Cheng, Department of Radiology, Pamela Youde Nethersole Eastern Hospital, Hong Kong SAR, China  
Email: [cwt413@ha.org.hk](mailto:cwt413@ha.org.hk)

Submitted: 10 January 2024; Accepted: 1 November 2024.

Contributors: BWTC and JHMC designed the study. BWTC, JHMC and KHC acquired the data. All authors analysed the data. BWTC drafted the manuscript. All authors critically revised the manuscript for important intellectual content. All authors had full access to the data, contributed to the study, approved the final version for publication, and take responsibility for its accuracy and integrity.

Conflicts of Interest: All authors have disclosed no conflicts of interest.

Funding/Support: This study received no specific grant from any funding agency in the public, commercial, or not-for-profit sectors.

Data Availability: All data generated or analysed during the present study are available from the corresponding author on reasonable request.

Ethics Approval: The study was approved by the Central Institutional Review Board of Hospital Authority, Hong Kong (Ref No.: CIRB-2023-199-2). A waiver of patient consent was obtained from the Board due to the retrospective nature of the study.

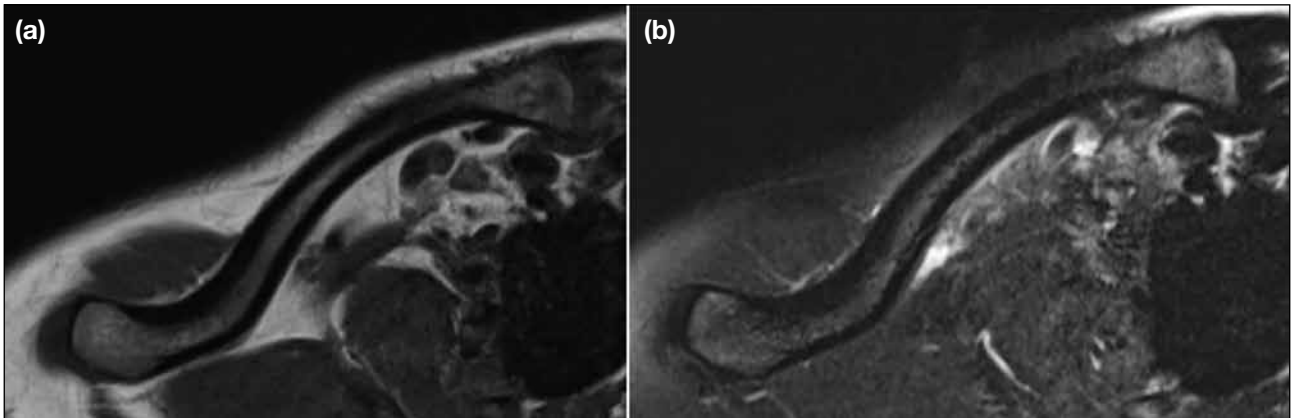


**Figure 1.** Anatomy of the clavicle. (a) Axial-oblique T1-weighted and (b) short-tau inversion recovery magnetic resonance images of the right clavicle demonstrate the S-shaped bone with a large medial end, a tubular mid-portion, and flaring of the lateral end.

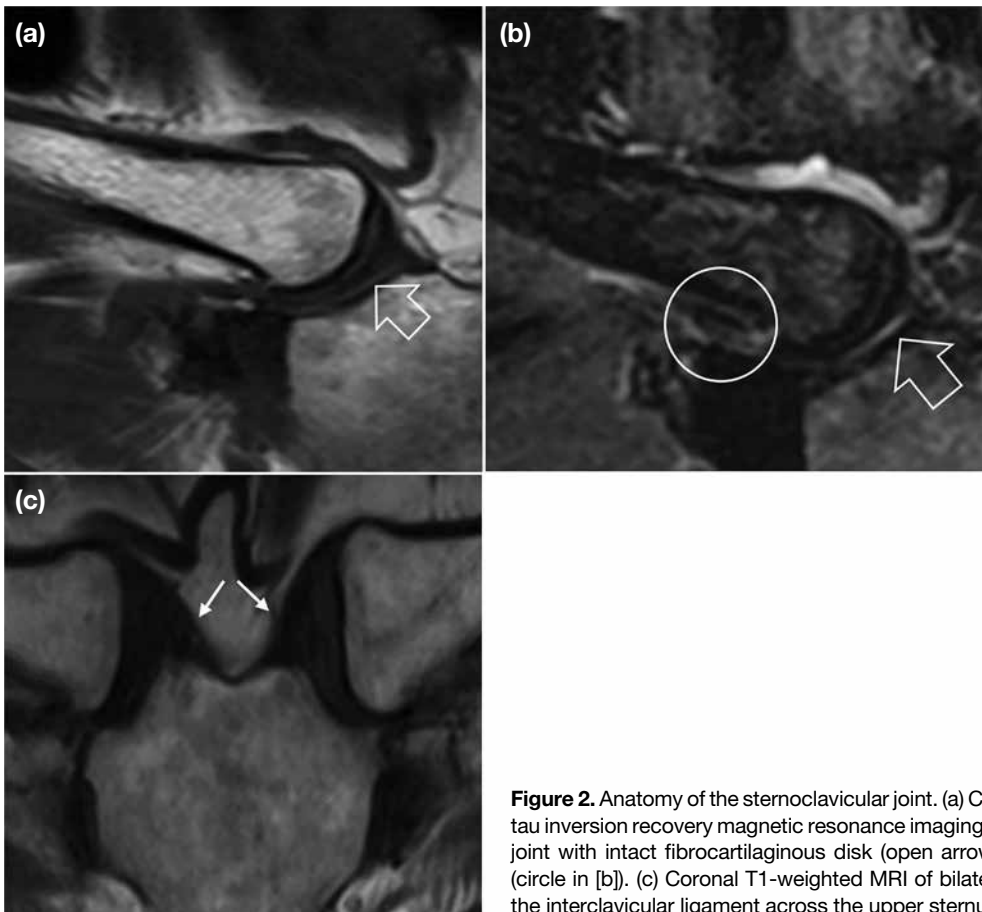


**Figure 2.** Anatomy of the sternoclavicular joint. (a) Coronal T1-weighted and (b) short-tau inversion recovery magnetic resonance imaging (MRI) of the right sternoclavicular joint with intact fibrocartilaginous disk (open arrows) and costoclavicular ligament (circle in [b]). (c) Coronal T1-weighted MRI of bilateral sternoclavicular joints shows the interclavicular ligament across the upper sternum (arrows).

disease that mainly affects midline skeletal structures, with features including hypoplasia or aplasia of the clavicles, large fontanelles, multiple Wormian bones,

a widened pubic symphysis, and supernumerary teeth (Figure 4). Eight cases of cleidocranial dysostosis were identified during the review period.

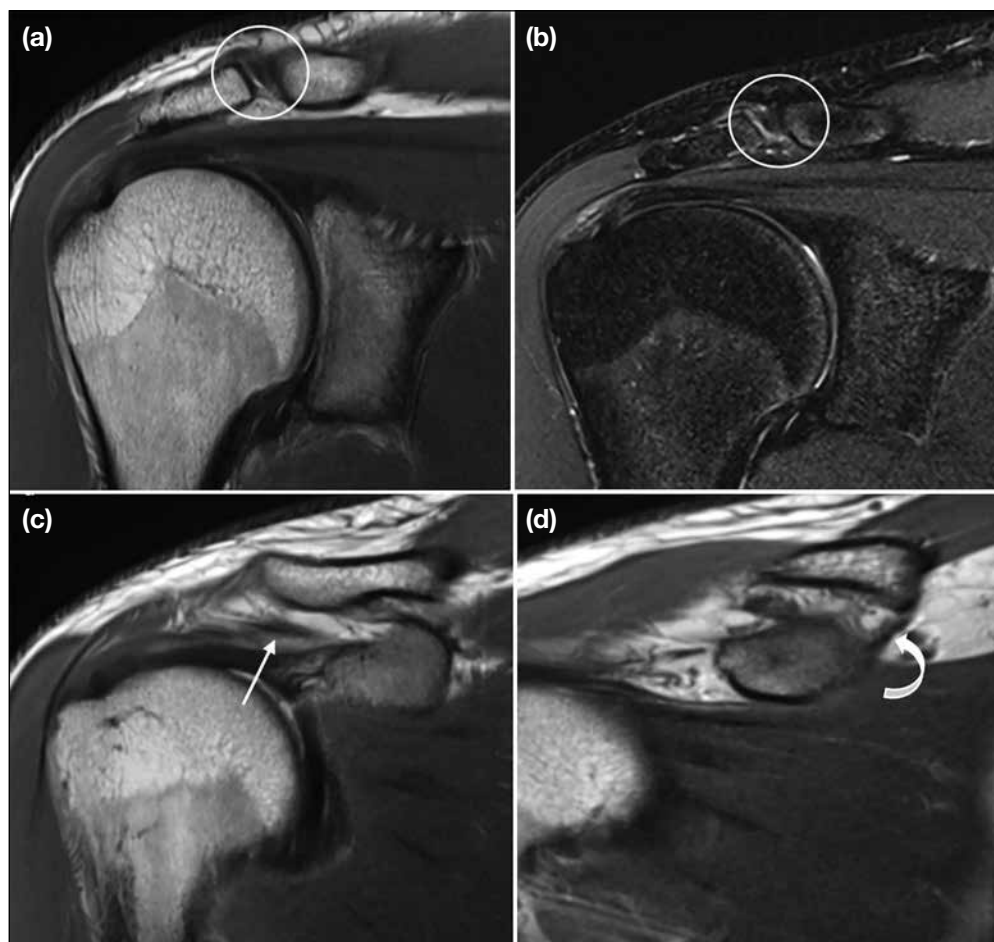


**Figure 3.** Anatomy of the acromioclavicular joint. (a) Coronal proton density (PD)-weighted and (b) T2-weighted fat-suppressed magnetic resonance imaging (MRI) of the right acromioclavicular joint with normal acromioclavicular joint capsule (circles), which cannot be differentiated from the acromioclavicular ligaments on routine MRI. (c, d) Coronal PD-weighted MRI of the right shoulder demonstrates ligaments around the distal clavicle. The coracoacromial ligament is located most laterally (arrow in [c]). The trapezoid portion of the coracoclavicular ligament is located more medially and inserts onto the inferior margin of the lateral clavicle; the conoid portion (curved arrow in [d]) is the most medial and vertically oriented.

### Articular Infection

Septic arthritis of the sternoclavicular joint is uncommon and is usually monoarticular with an insidious onset.<sup>4</sup> Radiological features on radiographs and computed tomography (CT) include subarticular erosions, joint space widening, and fluid collections. Magnetic resonance imaging (MRI) features include bone marrow oedema, bone destruction, joint effusion, and inflammatory changes of the surrounding soft tissue. Both CT and MRI are useful for early diagnosis and assessment of complications such as associated osteomyelitis and retrosternal/chest wall abscesses that may require surgical treatment.

### Inflammation

Spondyloarthropathies such as ankylosing spondylitis and psoriasis can affect the sternoclavicular joint. Radiographic and CT features include bone erosions,

partial or complete fusion of the joint, and hyperostosis surrounding the joint<sup>2</sup> (Figures 5-7). Rheumatoid arthritis may be accompanied by pannus formation with bony erosions on imaging.

The SAPHO (synovitis, acne, pustulosis, hyperostosis, and osteitis) syndrome is an inflammatory condition with aseptic osteoarticular involvement and characteristic skin lesions. In adults, it usually involves the anterior chest wall (60%-95%), particularly the sternocostoclavicular junction, followed by the axial skeleton, such as the spine and sacroiliac joints. Features of SAPHO on radiographs and CT include bony sclerosis, cortical thickening, and narrowing of the medullary canal. Adjacent changes include joint space narrowing and periarticular osteopenia, as well as ligamentous ossification with bony bridging across the joint. CT is good for detecting the osteoarticular manifestations, while MRI is sensitive in

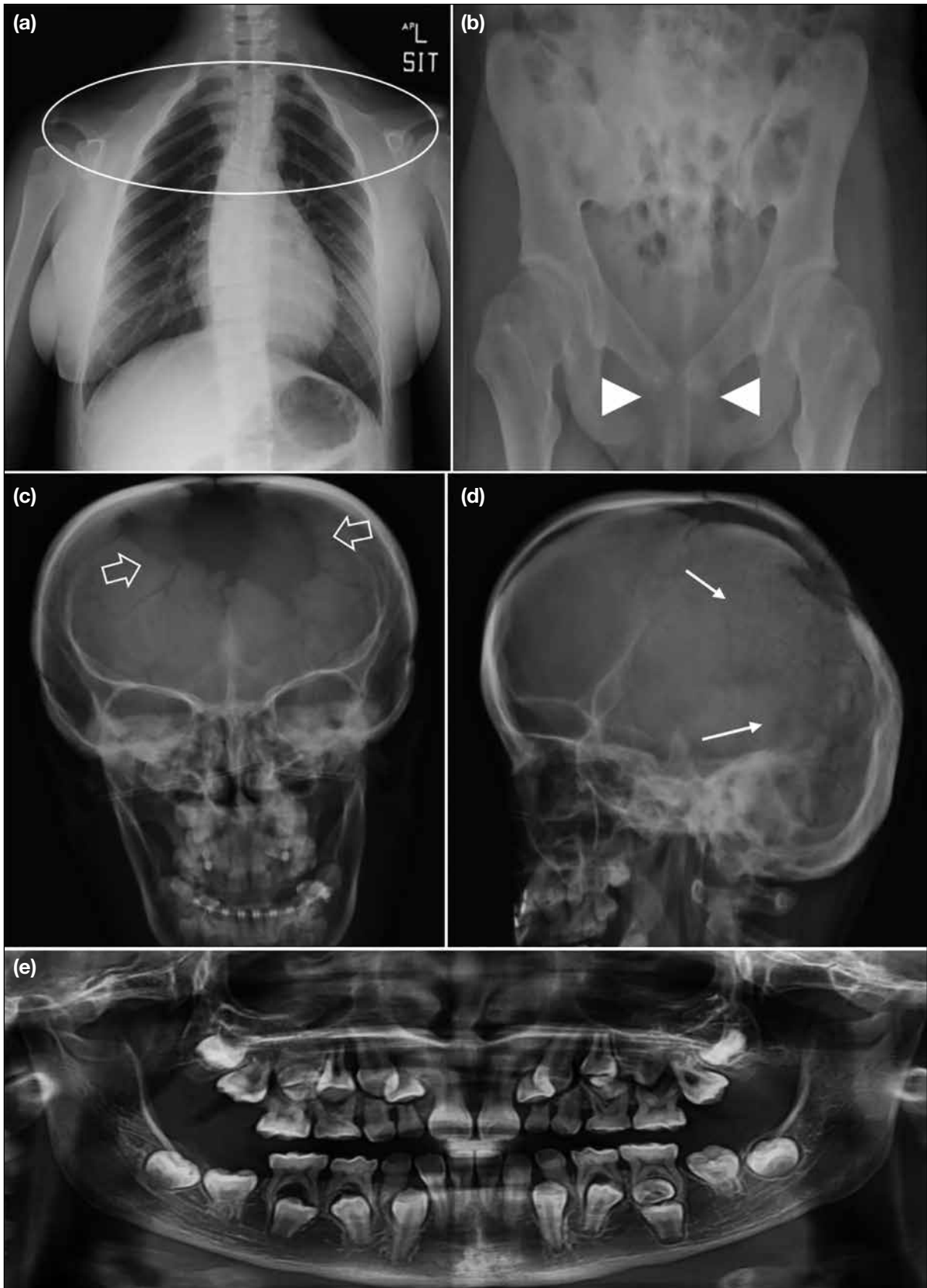


**Figure 4.** A case of cleidocranial dysostosis. (a) Chest X-ray demonstrates aplasia of bilateral clavicles (ellipse). (b) Pelvic X-ray demonstrates widening of pubic symphysis (arrowheads). Frontal (c) and lateral (d) skull X-rays demonstrate widened sagittal suture (open arrows in [c]) and multiple Wormian bones (arrows in [d]). (e) Orthopantomogram demonstrates supernumerary teeth.



**Figure 5.** Two cases of spondyloarthropathy of the sternoclavicular joint. (a-c) First case. (a) Coronal and (b) axial computed tomography (CT) bone window images of bilateral sternoclavicular joints in a patient with known ankylosing spondylitis. The right sternoclavicular joint demonstrates osseous fusion (circles), while the left shows hyperostosis with mild bone erosions and subchondral sclerotic changes (arrows). (c) X-ray of the cervical spine demonstrates bamboo spine. (d-f) Second case. (d) Coronal and (e) axial-oblique CT bone window images of the left sternoclavicular joint demonstrate hypertrophic change, bone erosions and sclerosis (open arrows) in a case of known psoriasis. (f) Pelvic X-ray demonstrates bony ankylosis of bilateral sacroiliac joints (arrowheads).

detecting early disease with bone and soft tissue oedema. On bone scintigraphy, SAPHO in the anterior chest wall typically manifests as the ‘bull’s head’ sign, with mostly symmetrical increased uptake in the sternoclavicular regions.<sup>5</sup> The radiological differential diagnosis includes sternoclavicular osteoarthritis, condensing osteitis of the clavicle, osteonecrosis, and septic arthritis (Figure 6). Six cases of SAPHO were identified during the review period.

### Degenerative Joint Disease

Osteoarthritis is a common cause of pain at the AC and sternoclavicular joints (Figures 7-9). Radiological features include narrowing of the joint space, marginal osteophytes, capsular hypertrophy, subchondral sclerosis, cysts, and bone marrow oedema.

A chronic large full-thickness supraspinatus tendon tear can lead to superior migration of the humeral head,

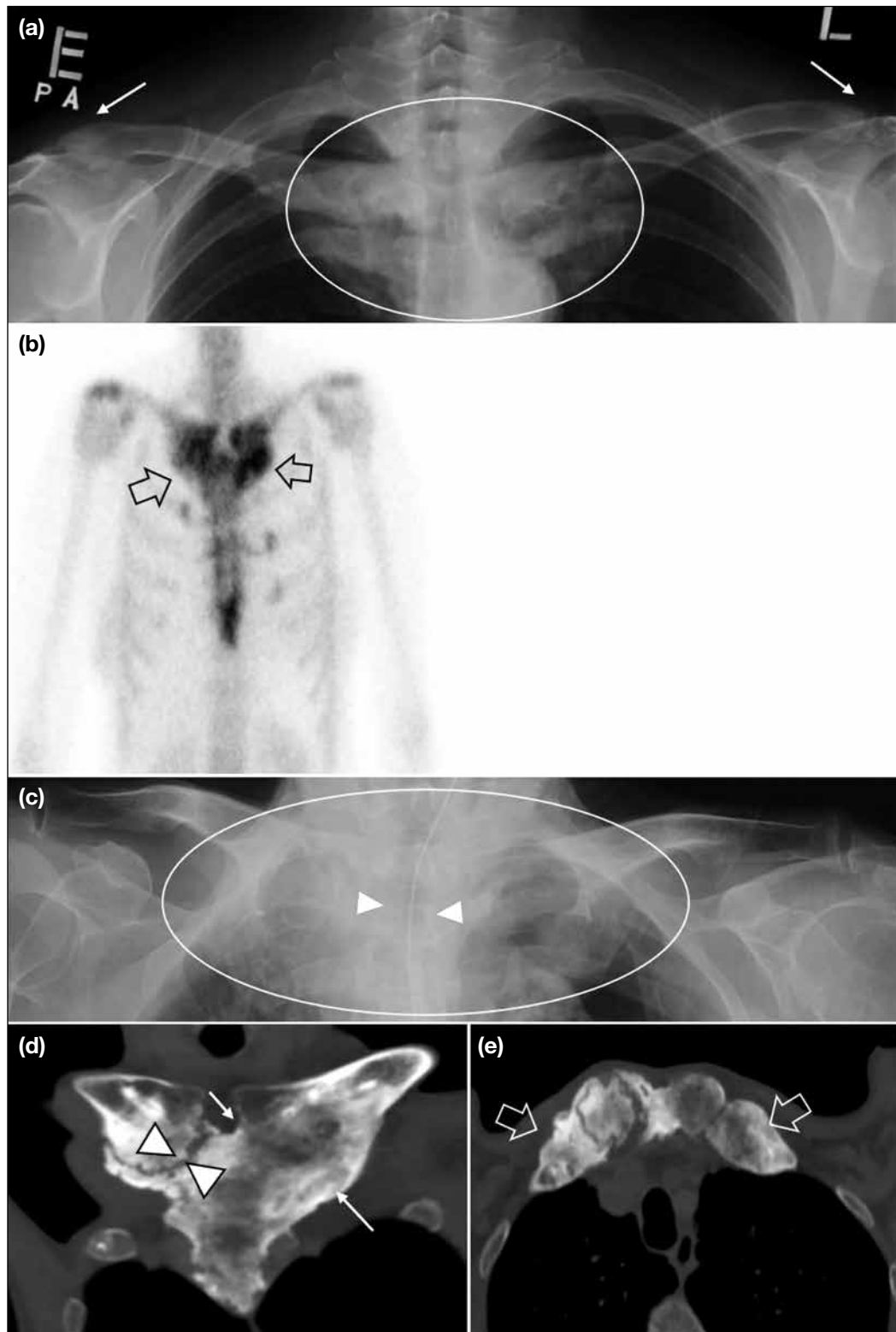


**Figure 6.** Two cases of the SAPHO (synovitis, acne, pustulosis, hyperostosis, and osteitis) syndrome. (a, b) First case. (a) Radiograph of the clavicles demonstrates prominent hyperostosis in both sternoclavicular joints (circle), more on the right, and sclerosis in both distal clavicles (arrows). (b) Bone scintigraphy demonstrates diffusely increased tracer uptake in both sternocostoclavicular junctions and medial clavicular ends (open arrows), associated with hyperostosis, compatible with the 'bull's head' sign. (c-e) Second case. (c) X-ray demonstrates hyperostosis of both medial clavicles (circle). A Ryles tube is noted (arrowheads). (d) Coronal and (e) axial bone window computed tomography images demonstrate corresponding significant sternoclavicular hyperostosis (open arrows in [e]), marked joint space narrowing on the right with cortical irregularities (arrowheads in [d]) and complete ankylosis on the left (arrows in [d]).

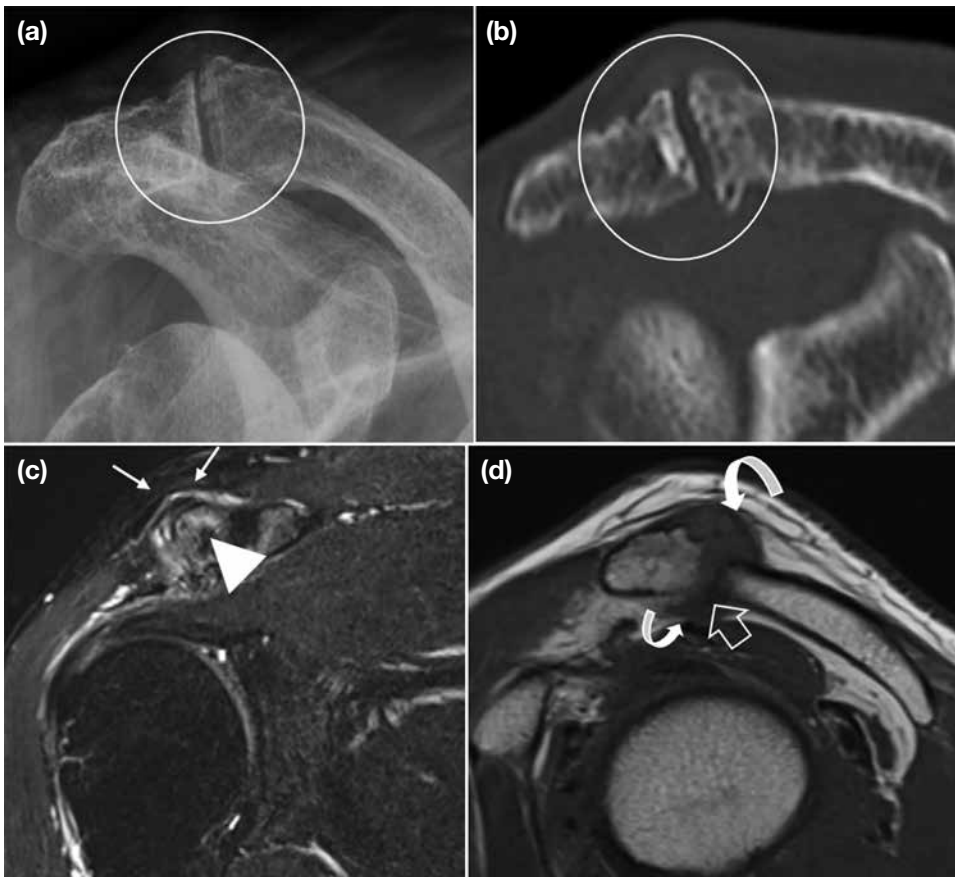


**Figure 7.** A case of osteoarthritis of the right acromioclavicular joint. (a) Radiograph and (b) coronal bone window computed tomography of the acromioclavicular joint demonstrate osteoarthritis with joint space narrowing, marginal osteophytes, subchondral sclerosis and cysts (circles). (c) Coronal short-tau inversion recovery magnetic resonance imaging (MRI) of the acromioclavicular joint shows subchondral bone marrow oedema (arrowhead) and thickened superior capsule (arrows). (d) Sagittal T1-weighted MRI shows inferior osteophyte of the acromion (open arrow) and capsular hypertrophy (curved arrows) of the acromioclavicular joint mildly indenting the supraspinatus tendon.

which may erode the subacromial-subdeltoid bursa and inferior AC capsule, forming a communication between the glenohumeral and AC joints. This may lead to a sizeable fluid pouch over the AC joint, giving rise to the geysers sign (Figure 8). During the review period, six such cases were identified.

### Trauma

Clavicular fractures (Figures 10-12) are common and represent 2.6% to 5% of all fractures, with the vast majority occurring in the mid clavicle (69%-82%).<sup>6</sup> Apart from location, alignment of the clavicle with the AC and sternoclavicular joints should be assessed, since malalignment may signify significant ligamentous injury.

AC joint injury is a common injury, occurring in 9% to 12% of shoulder injuries. The Rockwood classification is

the most widely used classification system for AC joint injuries. It is classified into six types, depending on the direction and degree of clavicular displacement, which correlates with the severity of injury and involvement of the AC and coracoclavicular ligaments, and the deltotracheal complex (Table).

Sternoclavicular joint dislocations are classified as anterior or posterior, and posterior dislocation has potentially serious complications due to the risk of injury to mediastinal structures such as the trachea and great vessels. On non-rotated radiographs, a difference in the relative craniocaudal positions of the medial clavicles exceeding 50% of the width of the clavicular heads suggests dislocation. However, diagnosis by radiographs may be difficult due to anatomical superimposition. CT is required for definitive diagnosis and to assess potential mediastinal injury.

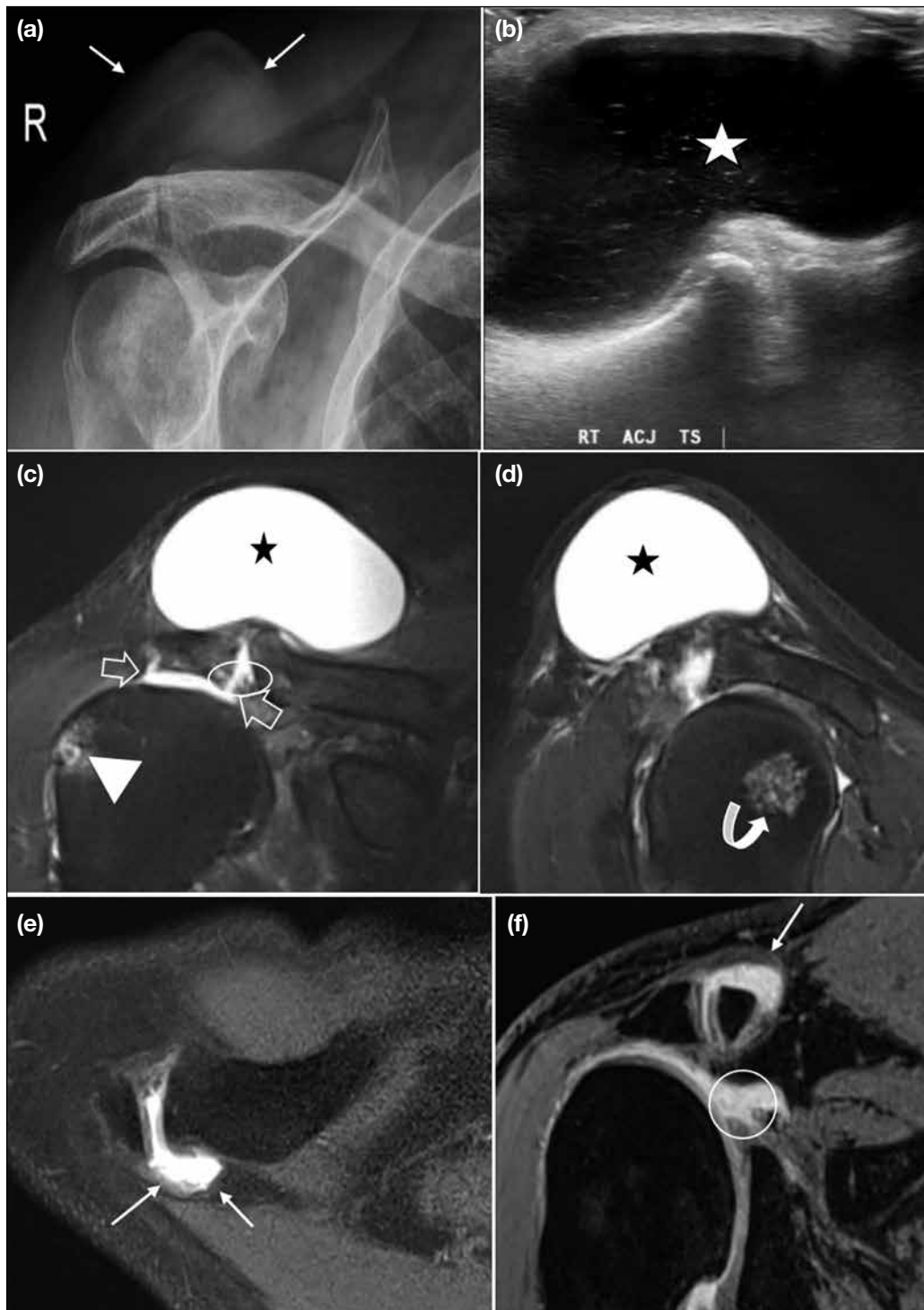


**Figure 8.** Two cases of complete chronic supraspinatus tear with geysers sign. (a-d) First case. (a) Radiograph shows a soft tissue shadow (arrows) above the acromioclavicular joint with mild osteoarthritic change. Superior migration of the humeral head and subacromial acetabularisation are noted, highly suggestive of chronic supraspinatus tear. (b) Transverse ultrasound demonstrates a cystic lesion with low-level echoes above the acromioclavicular joint (white star). Corresponding coronal (c) and sagittal (d) T2-weighted fat-suppressed magnetic resonance images show complete supraspinatus tendon tear (open arrows in [c]) with uncovering and superior migration of the humeral head, disrupted inferior capsule (circle in [c]), and a well-defined homogenous cystic lesion resembling the geysers sign (black stars). Incidental findings include a subcortical bone cyst (arrowhead in [c]) and enchondroma (curved arrow in [d]) at the humeral head. (e, f) Second case. (e) Axial and (f) coronal T1-weighted fat-suppressed volumetric interpolated breath-hold examination magnetic resonance arthrogram images of the right shoulder demonstrate a full-thickness tear of the supraspinatus-infraspinatus interdigitation (circle in [f]) with superior migration of the humeral head. There is contrast extension via the subacromial-subdeltoid bursa to the acromioclavicular joint (arrows).

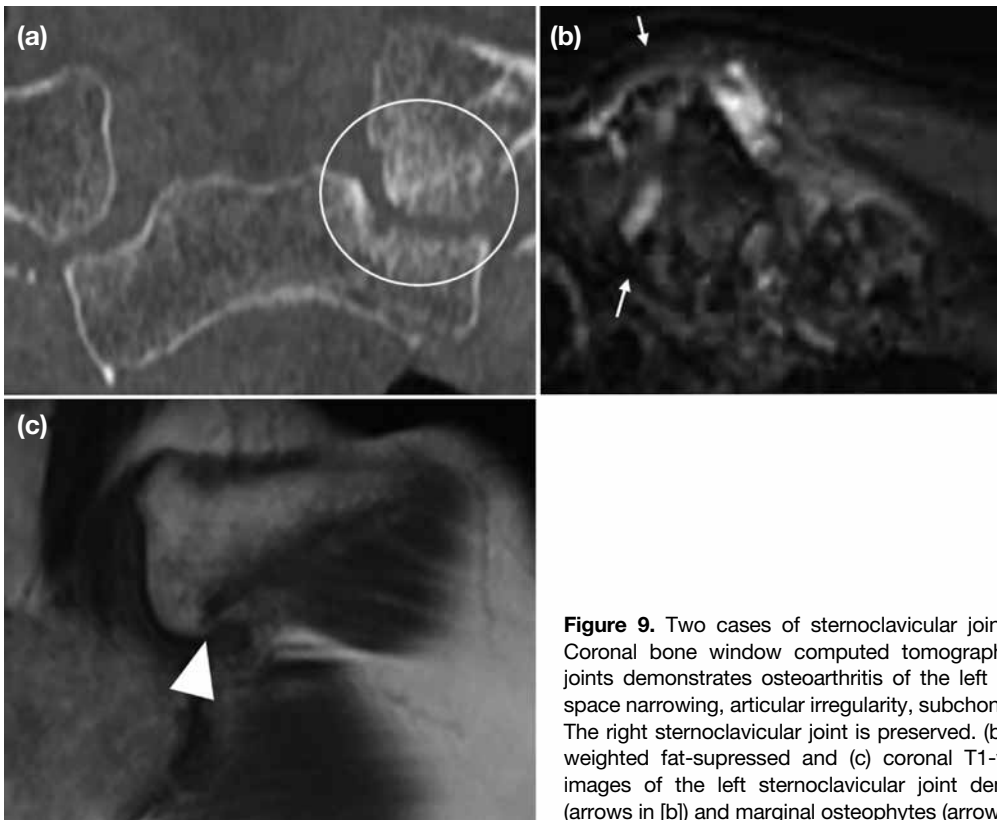


**Figure 9.** Two cases of sternoclavicular joint osteoarthritis. (a) First case. Coronal bone window computed tomography of bilateral sternoclavicular joints demonstrates osteoarthritis of the left sternoclavicular joint with joint space narrowing, articular irregularity, subchondral sclerosis and cysts (circle). The right sternoclavicular joint is preserved. (b, c) Second case. (b) Axial T2-weighted fat-suppressed and (c) coronal T1-weighted magnetic resonance images of the left sternoclavicular joint demonstrate capsular thickening (arrows in [b]) and marginal osteophytes (arrowhead in [c]).

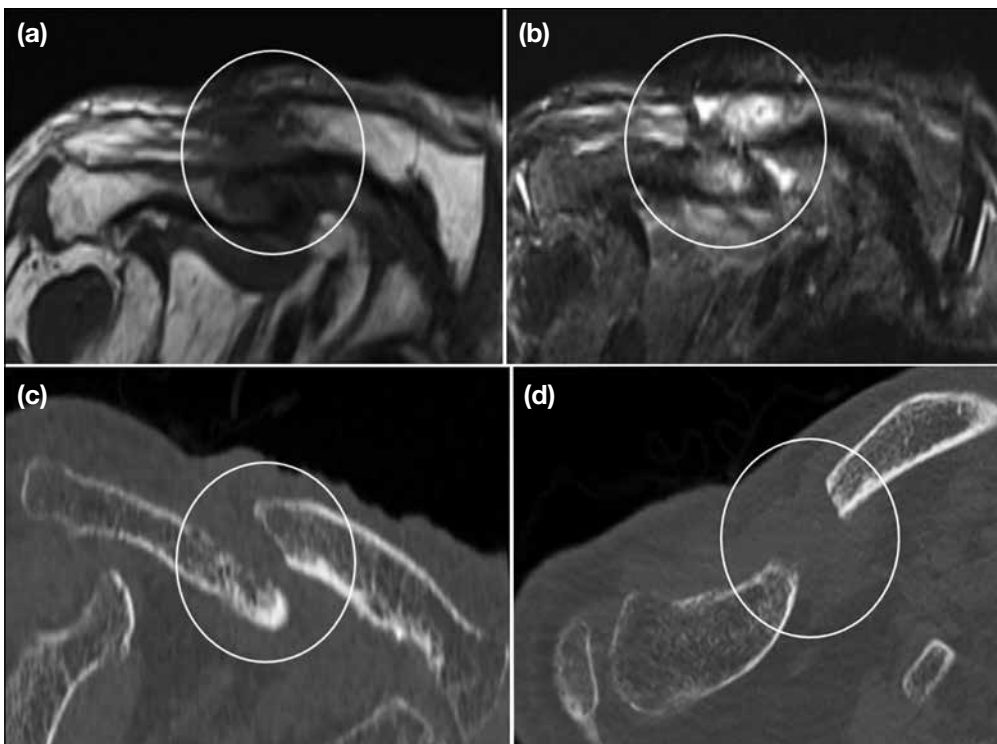


**Figure 10.** A case of right midclavicular fracture. (a) Coronal T1-weighted and (b) short-tau inversion recovery (STIR) magnetic resonance images demonstrate displaced midclavicular fracture (circles). T1-weighted hypointense, STIR hyperintense bone marrow change next to the fracture indicate posttraumatic change. (c) Coronal and (d) axial bone window computed tomography images show displaced midclavicular fracture (circles) with superior angulation and inferior displacement of the distal fragment.



**Figure 11.** Two cases of acromioclavicular joint injury. (a-d) First case. (a) Radiograph of the left acromioclavicular joint demonstrates slight superior displacement of the clavicle (arrows). (b-d) Sagittal and coronal T2-weighted fat-suppressed magnetic resonance imaging (MRI) of the left shoulder demonstrates increased signal in the coracoclavicular ligament (circle) and acromioclavicular ligament/joint capsule (open arrows), suggestive of Rockwood type II left acromioclavicular joint injury. (e-g) Second case. (e, f) Radiographs of the right acromioclavicular joint show markedly elevated clavicle with increased coracoclavicular distance, consistent with Rockwood type V right acromioclavicular joint injury. (g) Post-open reduction radiograph shows satisfactory joint alignment.

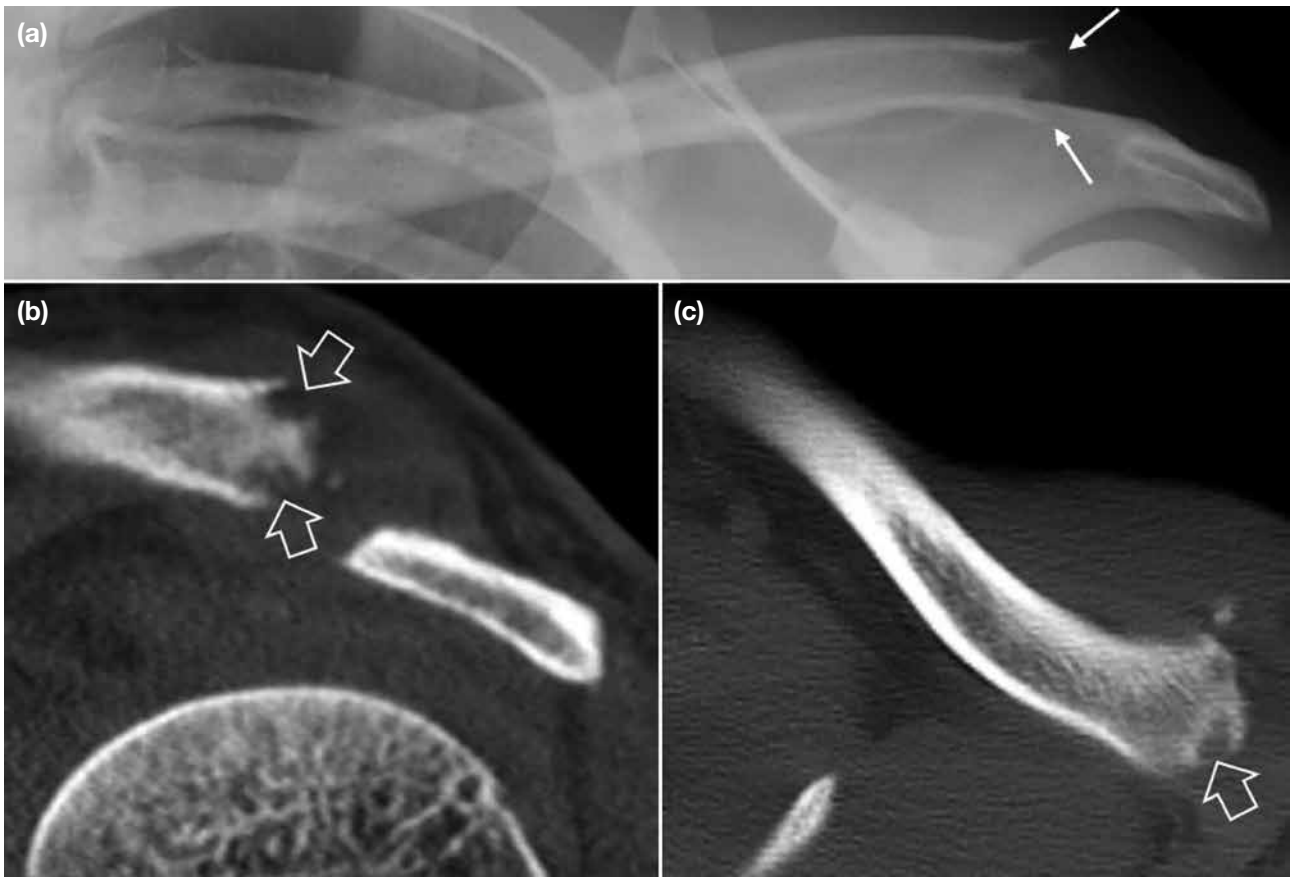


**Figure 12.** A case of posttraumatic left distal clavicle osteolysis. (a) Radiograph shows widening of the acromioclavicular joint with erosions at the lateral end of the clavicle (arrows). (b) Coronal and (c) axial bone window computed tomography demonstrates erosions over the lateral end of the clavicle (open arrows) with tiny adjacent osseous foci, and widening of the acromioclavicular joint with mild soft tissue swelling.

**Table.** Rockwood classification.

Type	AC ligament	CC ligament	Deltotrapezial complex	Radiographic appearance
I	Sprained	Intact	Intact	Normal
II	Ruptured	Sprained	Intact	Widened AC joint (>7 mm) with less than 25% clavicular elevation
III	Ruptured	Ruptured	Disrupted	Clavicle elevated above the superior border of acromion, increased CC distance by 25% to 100%
IV	Ruptured	Ruptured	Disrupted	Clavicle displaced posterior into the trapezius
V	Ruptured	Ruptured	Disrupted	Clavicle markedly elevated, increased CC distance by 100% to 300%
VI	Ruptured	Ruptured	Disrupted	Clavicle displaced inferior to coracoid process

Abbreviations: AC = acromioclavicular; CC = coracoclavicular.

### Distal Clavicle Osteolysis

Distal clavicle osteolysis (Figure 13) is painful bone resorption of the distal clavicle, most common in young adults with male predominance. It can be categorised into posttraumatic or overuse forms, which share identical imaging findings. Radiological features on radiographs

and CT include cortical irregularity, ‘flame-shaped’ bony resorption, and subchondral cysts involving the distal clavicle. MRI is most sensitive in demonstrating clavicular marrow oedema in the early phase of the disease. Effusion and capsular oedema are other features on MRI.

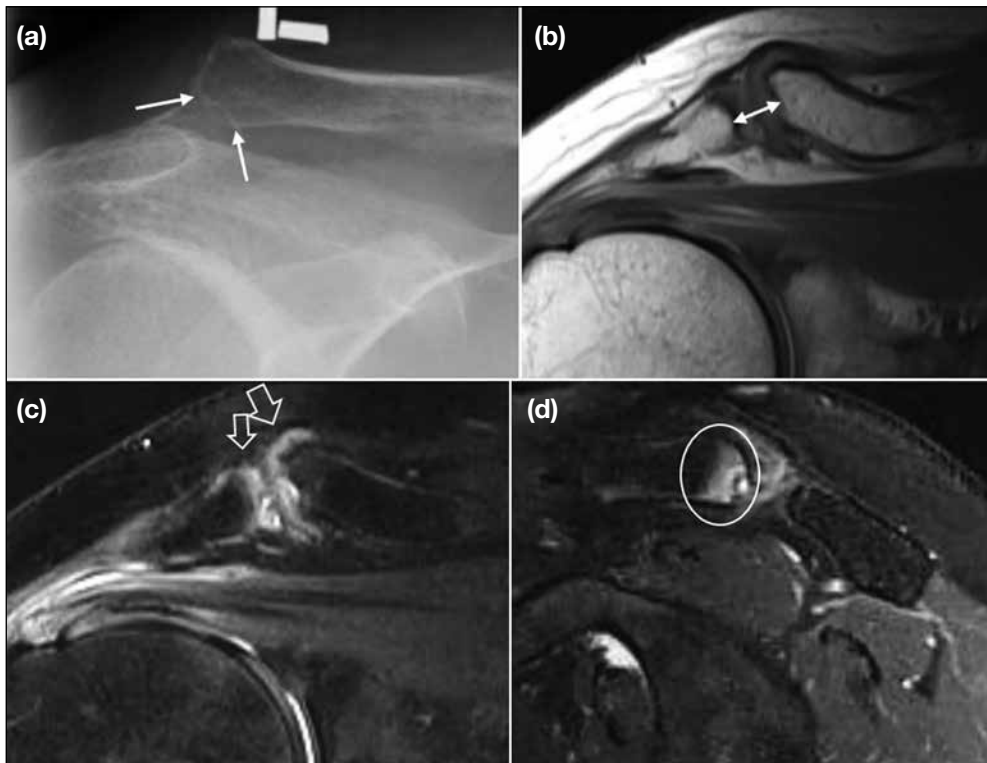


**Figure 13.** Posttraumatic right distal clavicle osteolysis. (a) Radiograph shows Rockwood type II injury with bone resorption at the inferior clavicular end (arrows). (b) Coronal proton density-weighted, (c) short-tau inversion recovery (STIR), and (d) sagittal STIR magnetic resonance images show widened joint space (double-head arrow in [b]) with capsular thickening (open arrows in [c]), and bone marrow oedema over the distal clavicle (circle in [d]).

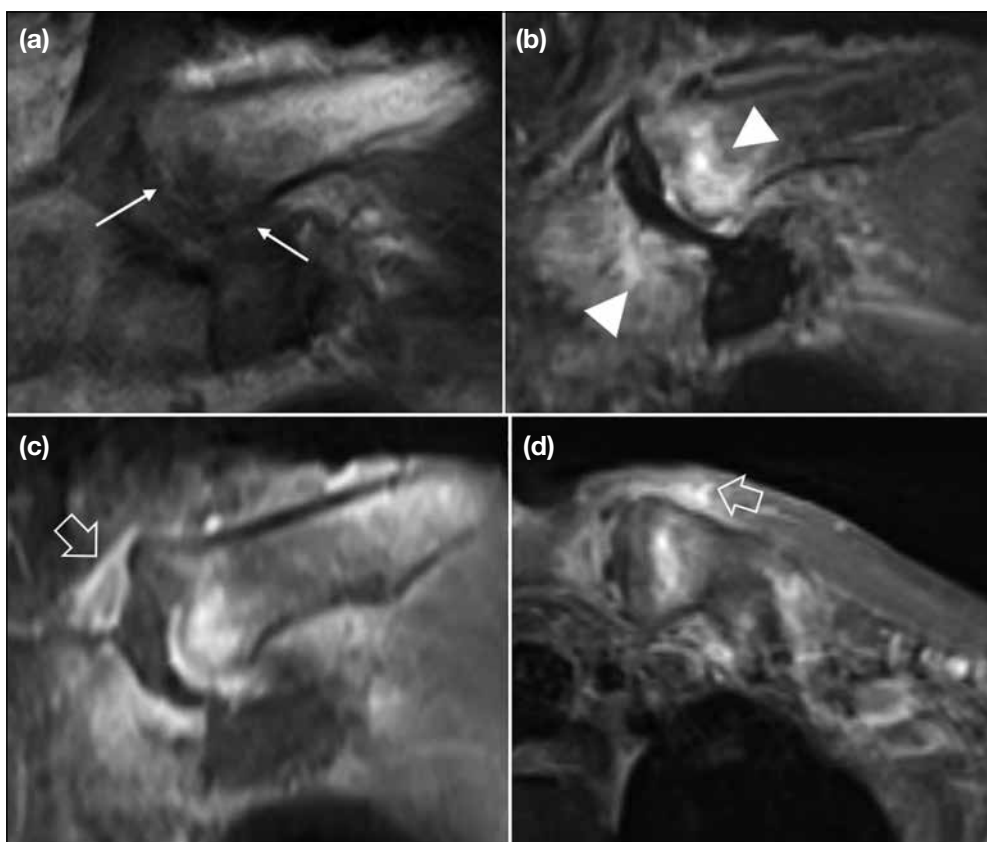


**Figure 14.** A case of septic arthritis of the left sternoclavicular joint. (a) Coronal T1-weighted, (b) short-tau inversion recovery, (c) coronal, and (d) axial post-contrast T1-weighted fat-suppressed magnetic resonance images show enhancing soft tissues (open arrows in [c] and [d]), bone marrow oedema of the medial clavicle and adjacent manubrium (arrowheads in [b]), and bony erosion of the medial end of the clavicle (arrows in [a]).

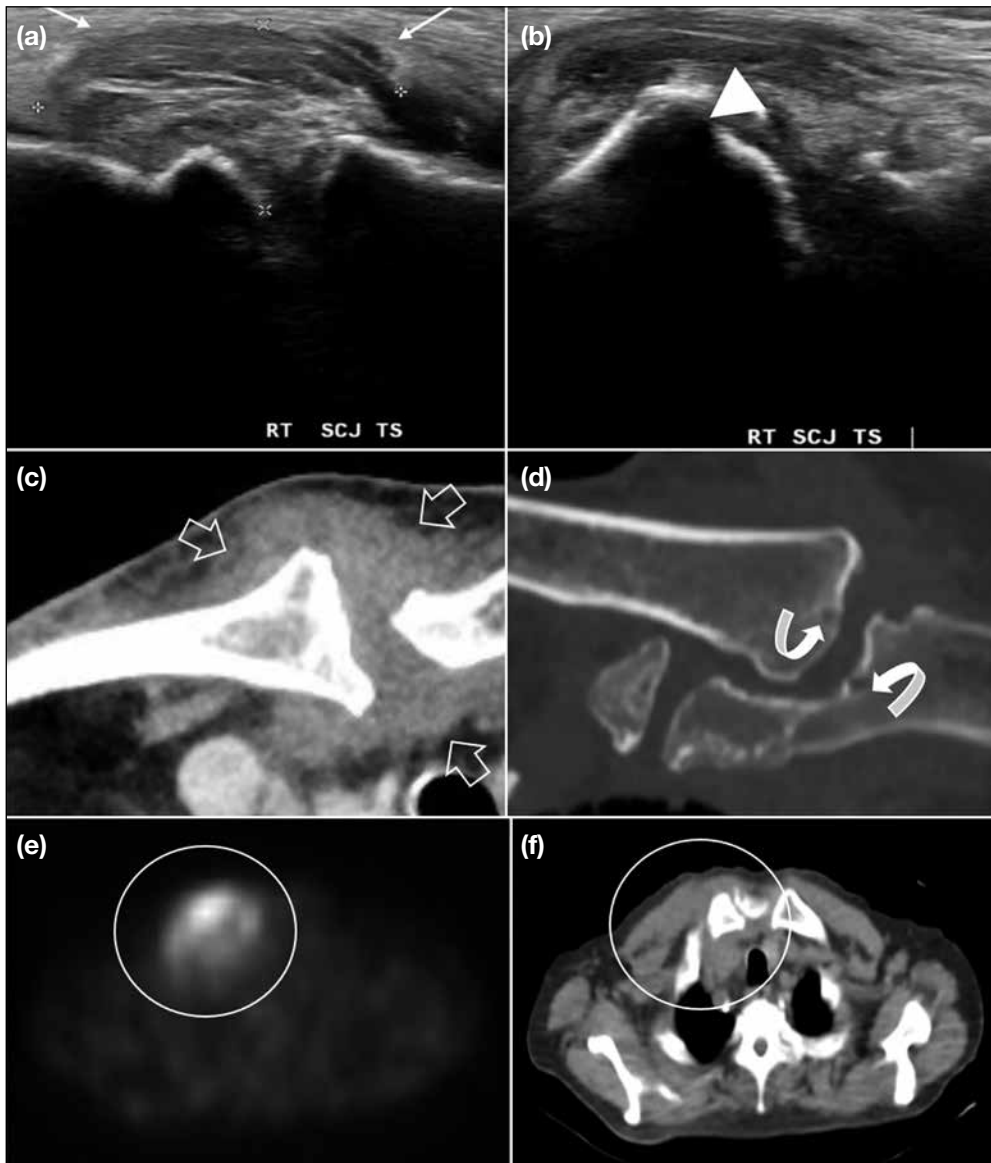


**Figure 15.** A case of *Staphylococcus aureus* septic arthritis of the right sternoclavicular joint. (a, b) Ultrasound shows gross capsular thickening of the joint (arrows in [a]) with cortical erosion over the articular surface of the clavicular head (arrowhead in [b]). (c) Axial soft tissue window and (d) coronal bone window computed tomography demonstrates enhancing soft tissue and fluid (open arrows in [c]) with subarticular erosions of the medial clavicle and adjacent manubrium (curved arrows in [d]). (e, f) Gallium-67 single-photon emission computed tomography/computed tomography of the thorax shows increased gallium activity involving the right sternoclavicular joint, adjacent right upper chest wall muscles with probable extension into the right medial clavicular head (circles).

The differential diagnoses of distal clavicle erosion include rheumatoid arthritis, hyperparathyroidism, and scleroderma.

### Non-Articular Infection

Radiological features of clavicular osteomyelitis on radiographs and CT include cortical erosion, regional osteopenia, periosteal reaction, and adjacent soft tissue swelling (Figures 14-16). On MRI, features of osteomyelitis typically include bone marrow oedema and surrounding soft tissue inflammatory change or

collection. With time, an intraosseous abscess may form, typically seen as a focal intramedullary T2-weighted hyperintensity with variable rim enhancement. Subsequently, other osteomyelitic features such as sequestrum, involucrum, and cloaca formation may also become apparent.

### Neoplasm

Bone tumours of the clavicle are rare, with a reported frequency of less than 1% of all bone tumours.<sup>6</sup> While primary bone tumour of the clavicle is uncommon,

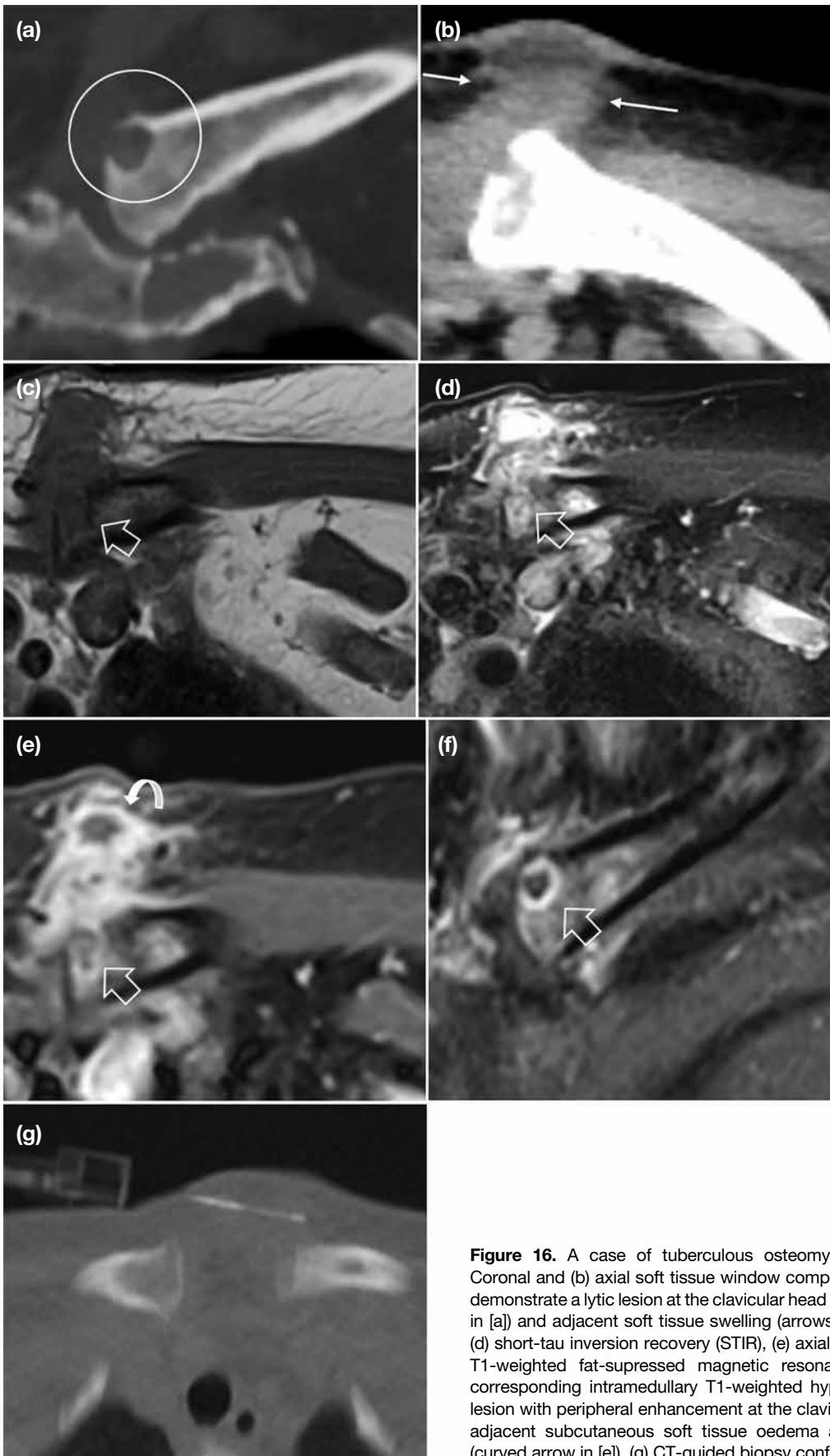


**Figure 16.** A case of tuberculous osteomyelitis of the left clavicle. (a) Coronal and (b) axial soft tissue window computed tomography (CT) images demonstrate a lytic lesion at the clavicular head with cortical destruction (circle in [a]) and adjacent soft tissue swelling (arrows in [b]). (c) Axial T1-weighted, (d) short-tau inversion recovery (STIR), (e) axial, and (f) coronal post-contrast T1-weighted fat-suppressed magnetic resonance images demonstrate a corresponding intramedullary T1-weighted hypointense, STIR hyperintense lesion with peripheral enhancement at the clavicular head (open arrows), and adjacent subcutaneous soft tissue oedema and rim-enhancing collection (curved arrow in [e]). (g) CT-guided biopsy confirms mycobacterial infection.

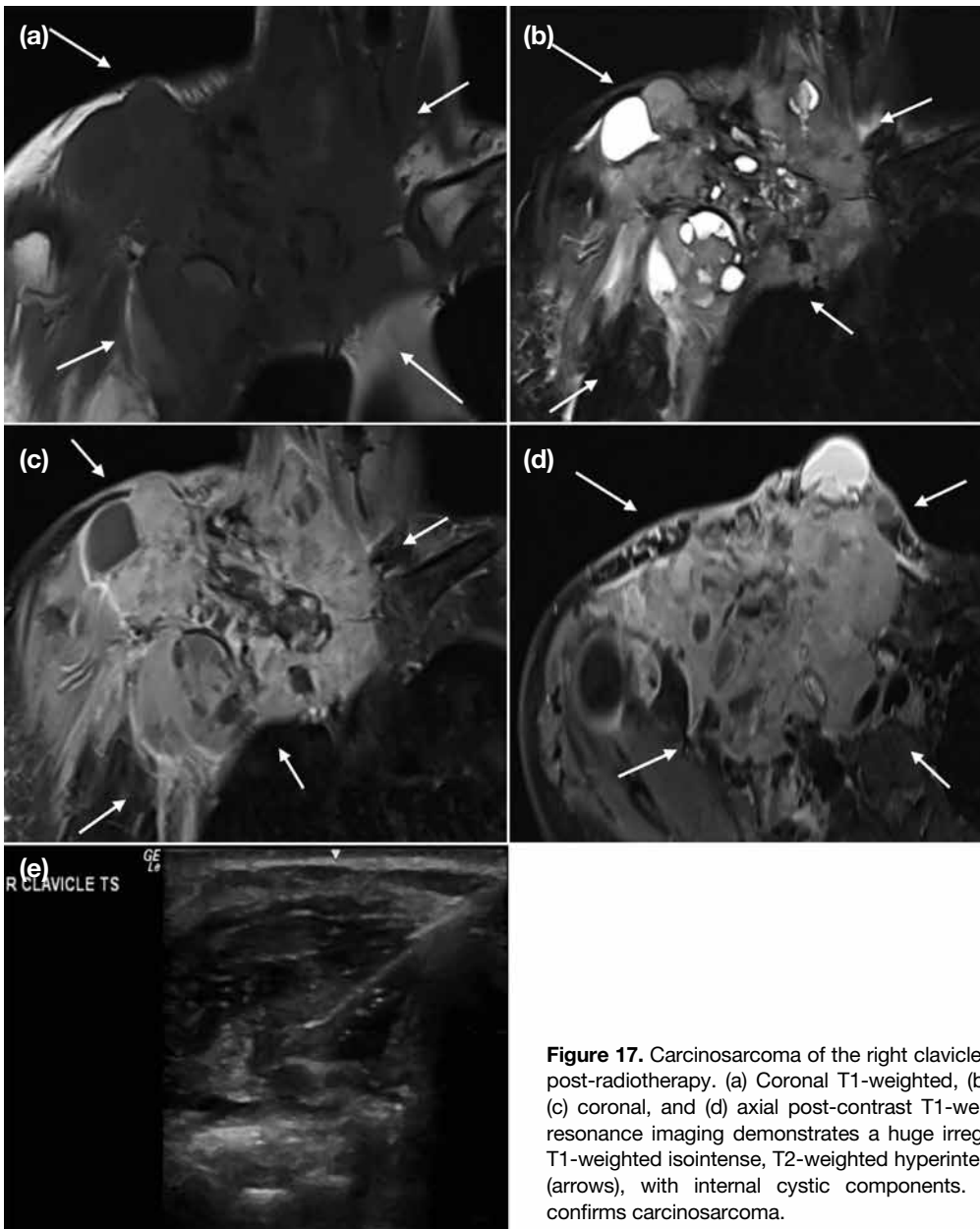


**Figure 17.** Carcinosarcoma of the right clavicle in a patient with breast cancer post-radiotherapy. (a) Coronal T1-weighted, (b) short-tau inversion recovery, (c) coronal, and (d) axial post-contrast T1-weighted fat-suppressed magnetic resonance imaging demonstrates a huge irregular heterogeneous enhancing T1-weighted isointense, T2-weighted hyperintense mass replacing the clavicle (arrows), with internal cystic components. (e) Ultrasound-guided biopsy confirms carcinosarcoma.

the majority are malignant and include plasmacytoma, osteosarcoma, and Ewing's sarcoma (Figures 17-19). Bone metastases can involve the clavicle, with breast, lung, and prostate cancer being the more common primaries. Radiological features of aggressive bone tumours on radiographs and CT include a wide zone of transition, cortical destruction, and periosteal reaction. On MRI, there is invariably marrow replacement, sometimes with bony destruction, extraosseous

extension, and perilesional oedema.

## CONCLUSION

The clavicle, AC joint, and sternoclavicular joint are important structures of the upper extremity. To make an accurate diagnosis for treatment guidance, radiologists need to be familiar with the normal anatomy as well as the radiological features of abnormalities across different imaging modalities.

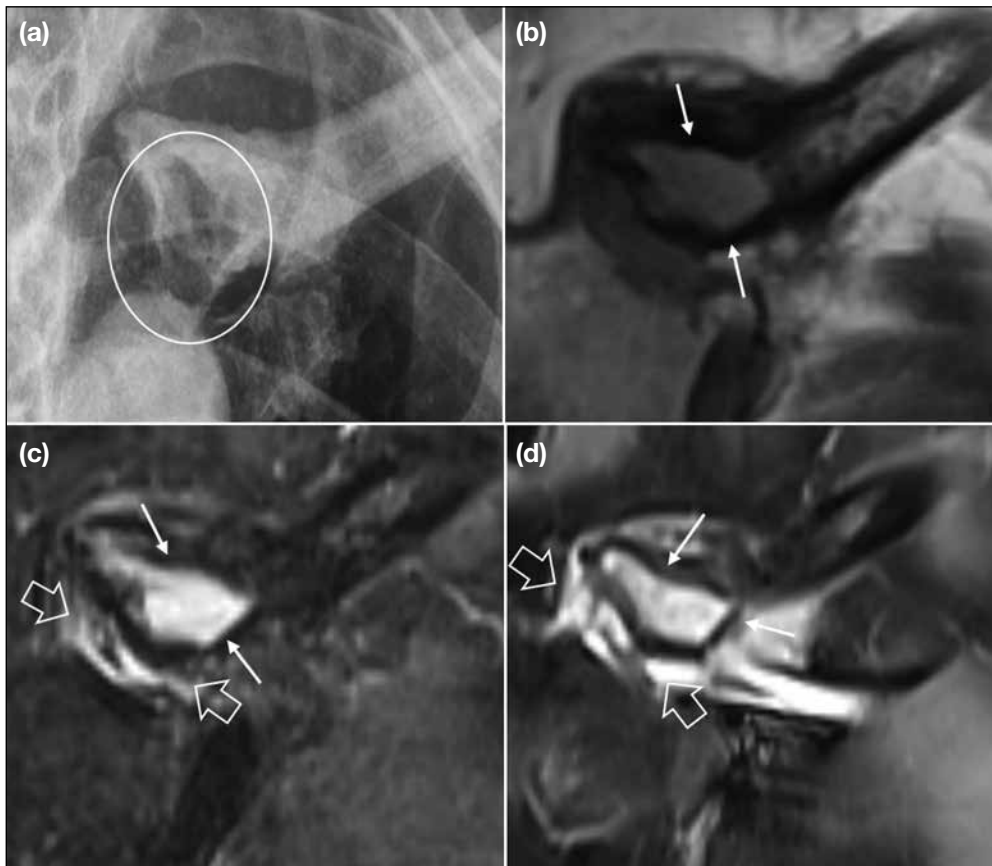


**Figure 18.** A case of myeloma at the left clavicle. (a) X-ray of the clavicle demonstrates a lytic lesion at the medial clavicle (circle). (b) Coronal T1-weighted, (c) short-tau inversion recovery (STIR), and (d) post-contrast T1-weighted fat-suppressed magnetic resonance images demonstrate a corresponding T1-weighted intermediate, STIR hyperintense and enhancing nodular lesion (arrows), expansile with mild adjacent soft tissue oedema and enhancement. Small joint effusion and capsule enhancement are noted (open arrows in [c] and [d]). Myeloma was confirmed by bone marrow aspiration.

## REFERENCES

1. Klein MA, Miro PA, Spreitzer AM, Carrera GF. MR imaging of the normal sternoclavicular joint: spectrum of findings. *AJR Am J Roentgenol.* 1995;165:391-3.
2. Olivier T, Kasprzak K, Herteleer M, Demondion X, Jacques T, Cotten A. Anatomical study of the sternoclavicular joint using high-frequency ultrasound. *Insights Imaging.* 2022;13:66.
3. Flores DV, Goes PK, Gómez CM, Umpire DF, Pathria MN. Imaging of the acromioclavicular joint: anatomy, function, pathologic features, and treatment. *Radiographics.* 2020;40:1355-82.
4. Restrepo CS, Martinez S, Lemos DF, Washington L, McAdams HP, Vargas D, et al. Imaging appearances of the sternum and sternoclavicular joints. *Radiographics.* 2009;29:839-59.
5. Depasquale R, Kumar N, Lalam RK, Tins BJ, Tyrrell PN, Singh J, et al. SAPHO: what radiologists should know. *Clin Radiol.* 2012;67:196-206.
6. Jeray KJ. Acute midshaft clavicular fracture. *J Am Acad Orthop Surg.* 2007;15:239-48.

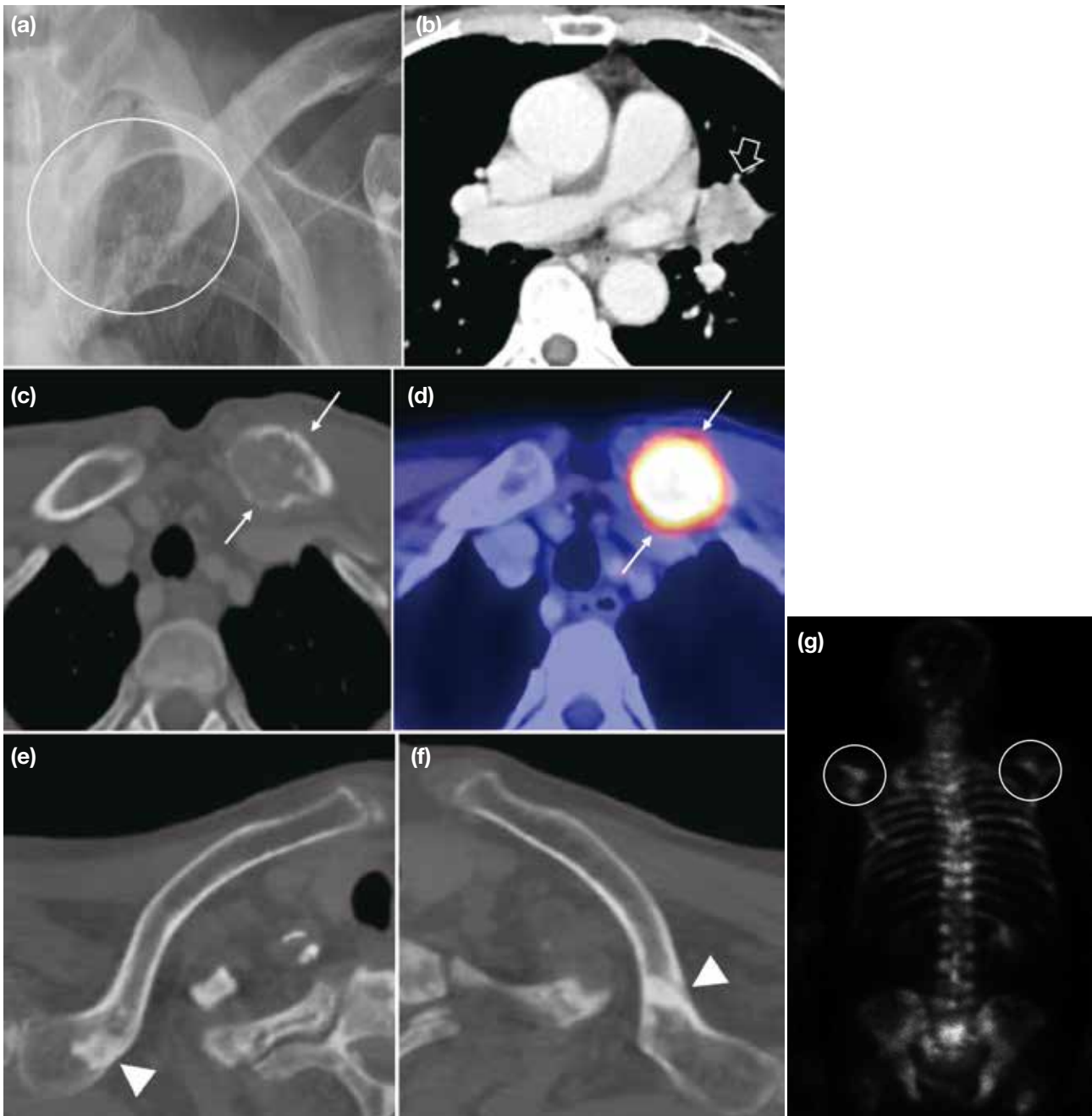


**Figure 19.** Two cases of bone metastases to the clavicle. (a-d) First case. (a) Radiograph of the left clavicle demonstrates an expansile destructive lytic lesion at the clavicular head with indistinct superior cortex (circle). (b) Axial soft tissue window computed tomography demonstrates a suspicious irregular hypoenhancing lung lesion in the lingula (open arrow), subsequently diagnosed as epidermal growth factor receptor mutation–positive lung carcinoma. (c) Axial bone window computed tomography (CT) and (d) positron emission tomography/CT demonstrate an expansile destructive lesion in the left clavicular head with pathological fracture and increased  $^{18}\text{F}$ -fluorodeoxyglucose uptake (arrows), compatible with bone metastasis. The right clavicular head is unremarkable. (e-g) Second case. (e, f) Axial bone window CT of bilateral clavicles of a patient with known prostate cancer demonstrate sclerotic lesions in the distal clavicle diaphyses (arrowheads). (g) Bone scan demonstrates innumerable foci of increased uptake, including the corresponding distal clavicles (circles), indicating disseminated bone metastasis.